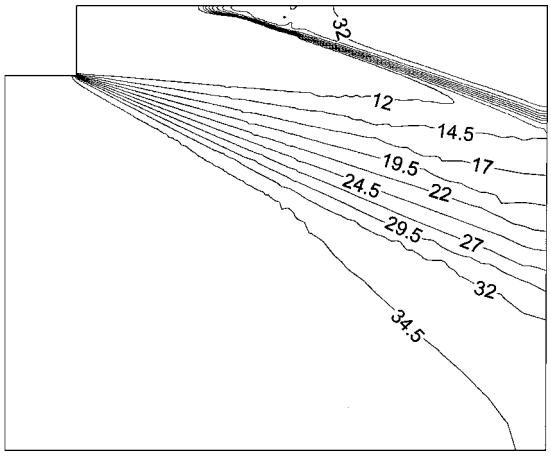

Fig. 6 Pressure contour obtained on the adaptive mesh Fig. 5.

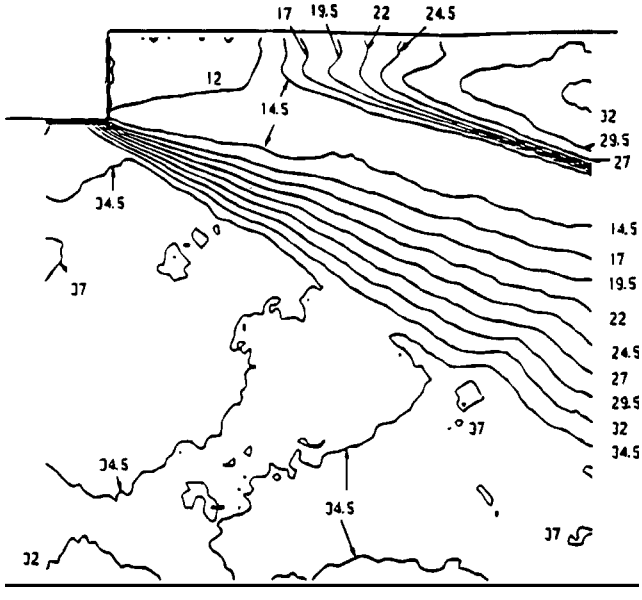

Fig. 7 Pressure contour obtained in the experiment.[2]

to that obtained in the experiment[2] (see Fig. 7). Based on the comparison, it is indicated that the present result can accurately capture the structure of Prandtl–Meyer expansion wave and oblique shock wave.

Conclusion

In the present work a solution-adaptive solver is presented to investigate the supersonic flow over a backward-facing step on mixed quadrilateral-triangular mesh. This solver incorporates the locally implicit scheme, two-level refinement procedure, and a modified error indicator. In a Cartesian coordinate system the Euler equations are solved. Based on the comparison of adaptive meshes obtained using four different error indicators, the modified error indicator can incorporate the advantages and avoid the disadvantages of the other three error indicators, which are $|\nabla\rho|$, $|\nabla M|$, and $|\nabla\omega|$. According to the adaptive mesh obtained using the modified error indicator, the structure of backstep corner vortex, expansion wave, and oblique shock wave is distinctly captured.

Acknowledgment

Support by the National Science Council of the Republic of China under Contract NSC 89-2212-E-150-016 is gratefully acknowledged.

References

[1]Loth, E., Kailasanath, K., and Lohner, R., "Supersonic Flow over an Axisymmetric Backward-Facing Step," *Journal of Spacecraft and Rockets*, Vol. 29, No. 3, 1992, pp. 352–359.

[2]Hartfield, R. J., Hollo, S. D., and McDaniel, J. C., "Planar Measurement Technique for Compressible Flows Using Laser Induced Iodine Fluorescence," *AIAA Journal*, Vol. 31, No. 3, 1993, pp. 483–490.

[3]Halupovich, Y., Natan, B., and Rom, J., "Numerical Solution of the Turbulent Supersonic Flow over a Backward Facing Step," *Fluid Dynamics Research*, Vol. 24, No. 5, 1999, pp. 251–273.

[4]Venkatakrishnan, V., "Perspective on Unstructured Grid Flow Solvers," *AIAA Journal*, Vol. 34, No. 3, 1996, pp. 533–547.

[5]Hwang, C. J., and Wu, S. J., "Global and Local Remeshing Algorithms for Compressible Flows," *Journal of Computational Physics*, Vol. 102, No. 1, 1992, pp. 98–113.

[6]Webster, B. E., Shephard, M. S., Rusak, Z., and Flaherty, J. E., "Automated Adaptive Time-Discontinuous Finite Element Method for Unsteady Compressible Airfoil Aerodynamics," *AIAA Journal*, Vol. 32, No. 4, 1994, pp. 748–757.

[7]Hwang, C. J., and Fang, J. M., "Solution-Adaptive Approach for Unsteady Flow Calculations on Quadrilateral-Triangular Meshes," *AIAA Journal*, Vol. 34, No. 4, 1996, pp. 851–853.

[8]Yang, S. Y., "Adaptive Analysis of Oscillating Cascade Flows on a Quadrilateral-Triangular Mesh," *Journal of Propulsion and Power*, Vol. 15, No. 3, 1999, pp. 479–481.

[9]Hwang, C. J., and Liu, J. L., "Inviscid and Viscous Solutions for Airfoil/Cascade Flows Using a Locally Implicit Algorithm on Adaptive Meshes," *Journal of Turbomachinery*, Vol. 113, No. 4, 1991, pp. 553–560.

Effect of Reynolds Number on Pitot-Pressure Distributions in Underexpanded Supersonic Freejets

Hiroshi Katanoda,* Taro Handa,† Yoshiaki Miyazato,‡
Mitsuharu Masuda,§ and Kazuyasu Matsuo¶
Kyushu University, Fukuoka 816-8580, Japan

Nomenclature

D	=	nozzle-exit diameter
e_{mean}	=	time-averaged output voltage of a hot-wire probe
e_{rms}	=	root-mean-squared output voltage of a hot-wire probe
p	=	pressure
p_i	=	pitot pressure
Re_d	=	Reynolds number based on the nozzle-exit condition
r	=	radial distance from jet centerline
r_m	=	Mach disk radius
x	=	axial distance from nozzle exit
x_m	=	Mach disk location

Subscripts

b	=	ambient condition
01	=	plenum chamber condition

Received 1 March 2000; revision received 26 February 2001; accepted for publication 16 March 2001.

*Postdoctoral Student, Department of Energy and Environmental Engineering, Graduate School of Engineering Sciences; currently Lecturer, Department of Mechanical Systems and Environmental Engineering, The University of Kitakyushu, 1-1 Hibikino, Wakamatsu-ku, Kitakyushu City; katanoda@env.kitakyu-u.ac.jp.

†Research Associate, Department of Energy and Environmental Engineering, Graduate School of Engineering Sciences, 6-1 Kasuga-Koen, Kasuga City; handa@ence.kyushu-u.ac.jp.

‡Associate Professor, Department of Energy and Environmental Engineering, Graduate School of Engineering Sciences, 6-1 Kasuga-Koen, Kasuga City; miyazato@ence.kyushu-u.ac.jp.

§Professor, Department of Energy and Environmental Engineering, Graduate School of Engineering Sciences, 6-1 Kasuga-Koen, Kasuga City; masuda@ence.kyushu-u.ac.jp.

¶Professor, Department of Energy and Environmental Engineering, Graduate School of Engineering Sciences, 6-1 Kasuga-Koen, Kasuga City; matsuo@ence.kyushu-u.ac.jp.

I. Introduction

In a coal-fired thermal power plant a fireside surface of a boiler tube suffers with deposit produced by the combustion of coal. A sootblower is used to washes off deposit by supersonic jets.[1] The performance of the sootblower depends on impact force of the jet. In industrial applications the pressure measured by a pitot probe is regarded as a measure of impact force of a jet so that the efforts have been made to develop nozzles with a high pitot pressure.

Among numerous experimental works on the flow structure of supersonic free jets,[2] a few have addressed the pitot-pressure distribution in the far-downstream region of the underexpanded jets. Much work has also been done on the numerical simulation of the supersonic free jets.[3] These, however, did not give information on the behavior of the pitot pressure.

Present paper aims to address the pitot-pressure distributions in underexpanded free jets with emphasis on its anomalous recovery in the downstream region. It is found that the recovery is caused by the turbulent momentum transfer from the high-momentum region outside the slip surface created by the Mach disk to the central region of the jet where momentum is low because of the loss caused by the Mach disk.

II. Experimental Setup and Method

A low-density wind tunnel was used. The working gas was nitrogen. The gas in a high-pressure reservoir was supplied to the plenum chamber, where it was stagnated. The gas was then accelerated by a supersonic nozzle and discharged into the wind-tunnel vacuum chamber evacuated by vacuum pumps.

The axisymmetric nozzle with the exit Mach number of 2.0 was used. The nozzle had a supersonic part contoured by an approximate theory.[4] The jet flowfield was measured by a pitot probe. The tip of this probe had a 1.0-mm outer diameter, a 0.9-mm inner diameter, and was 30 mm in length. The hot-wire probe was used to measure the temporal fluctuations in the jet. The hot wire was an I type with 5 μm in diameter and 1.1 mm in length. Freejets include both transonic and high-subsonic regions, where the relation between the output and the physical quantity is unknown. We, therefore, used the output of the hot-wire probe as a measure of fluctuation in the jet.

Table 1 summarizes the experimental conditions. These pressure ratios correspond to the underexpanded flows for the present nozzles. The plenum chamber and backpressures were set within the accuracy of ±1.5%.

Table 1 Experimental conditions

p_{01}, kPa	p_{01}/p_b	Re_d
4	20	3.9×10^3
8	20	7.7×10^3
12	20	11.6×10^3

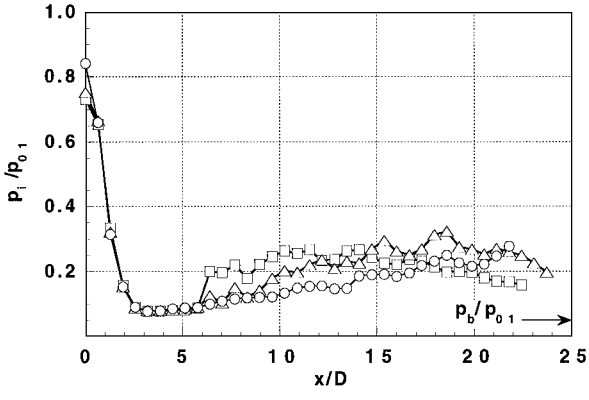

Fig. 1 Pitot pressure on the centerline (○, $Re_d = 3.9 \times 10^3$; △, $Re_d = 7.7 \times 10^3$; □, $Re_d = 11.6 \times 10^3$).

III. Results and Discussion

The pitot pressures of jets were measured along the centerline, and the results are plotted in Fig. 1. A peculiarity of this figure is that, with the increase in x/D, the pitot pressure recovers after taking the minimum value near $x/D \sim 3$. The empirical formula[5] gives that the Mach disk locations x_m/D is 2.7 for $p_{01}/p_b = 20$. The location of the minimum pitot pressure, therefore, corresponds to that of the Mach disk. The recovery of the pitot pressure downstream of the Mach disk is gradual for $Re_d = 3.9 \times 10^3$, whereas for $Re_d = 7.7 \times 10^3$ and 11.6×10^3 this recovery takes maximum values at $x/D = 16 \sim 18$. The spacial fluctuation of the pitot pressure is also observed downstream of the Mach disk; this is probably caused by the complicated expansion, compression, and/or shock waves generated in this region.

The fluctuation was measured by a hot-wire probe to clarify the cause of the recovery of pitot pressure. We express the fluctuation by $e_{\mathrm{rms}}/e_{\mathrm{mean}}$. A contour of the experimentally obtained $e_{\mathrm{rms}}/e_{\mathrm{mean}}$ is shown in Fig. 2. The data were taken at 24 axial locations with 21 radial positions at each x/D. The fluctuation is generated at two points, both are located at $x/D = 2 \sim 3$. Considering the experimental results obtained by Love et al.[6], the outer point corresponds to the jet boundary and the inner point to the periphery of the Mach disk. The latter region is the triple point at the stem of the Mach disk. The fluctuation, therefore, is probably generated by the shear layer on the bounding surface of the jet and also on the slip surface formed by the triple point. The fluctuation generated in these two regions then grows and also the shear layer thickens while traveling downstream. The fluctuation generated near the triple point extends to the jet centerline at $x/D = 8 \sim 10$.

Figure 3 shows $e_{\mathrm{rms}}/e_{\mathrm{mean}}$ as a function of x/D along with the location of the Mach disk obtained by the empirical formula.[5] According to this figure, the jet with $Re_d = 3.9 \times 10^3$ is quiescent, and no fluctuation is detected. As the Reynolds number increases, the fluctuation level increases, and the locations at which fluctuation starts to increase move upstream toward the Mach disk. As described in Fig. 2, the fluctuation is generated near the periphery of the Mach disk. Hence, the difference in the growth rate of the shear layer along the slip surface causes the starting point of the fluctuation to shift upstream with Re_d. Troutt and McLaughlin[2] studied experimentally the correctly expanded supersonic jets that included laminar to turbulent transition in the jet boundary, and they showed that the shear layer of the jet with $Re_d = 7.9 \times 10^3$ is thinner than that with $Re_d = 7 \times 10^4$. They thought that, in the shear layer, laminar to turbulent transition occurred at $x/D \sim 10$ and $x/D = 2 \sim 3$ for the jet with $Re_d = 7.9 \times 10^3$ and 7×10^4, respectively. This means that the shear layer becomes thick with the increase in Re_d if transition occurs. When the Reynolds number of the present experiments is considered, it seems probable that the transition occurred in the jet with $Re_d = 7.7 \times 10^3$ and 11.6×10^3. For that case the laminar to turbulent transition in the shear layer of the $Re_d = 11.6 \times 10^3$ jet occurred more upstream than the $Re_d = 7.7 \times 10^3$ jet, and this makes the shear layer for $Re_d = 11.6 \times 10^3$ thicker than that for 7.7×10^3. Consequently, the location at which the fluctuation starts to increase moves upstream toward the Mach disk with Re_d by the thicker shear layer along the slip surface. The comparison of Fig. 3 with Fig. 1 indicates that for $Re_d = 7.7 \times 10^3$ and 11.6×10^3, the fluctuation starts to increase almost at the same location where the pitot pressure begins to recover. This correspondence confirms that the pitot-pressure recovery is attributable to the turbulent momentum transfer from the high total pressure peripheral to the low total pressure central region downstream of the Mach disk.

Figure 4 is the radial distributions of the fluctuation (solid circles) along with those of the time-averaged pitot pressure (open circles), where r_m/D is the Mach disk radius experimentally obtained by Love et al.[6] For $Re_d = 3.9 \times 10^3$, which is not shown, almost no fluctuation is detected, and the jet seems laminar throughout the flowfield. This indicates that the viscous force transfers momentum from high total pressure peripheral to the low total pressure central part of the jet. On the other hand, for the jets with $Re_d = 7.7 \times 10^3$ and 11.6×10^3, at the immediate downstream

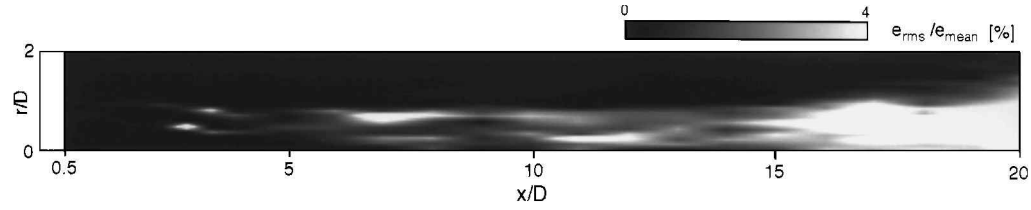

Fig. 2 Spatial distribution of turbulent fluctuation ($Re_d = 7.7 \times 10^3$).

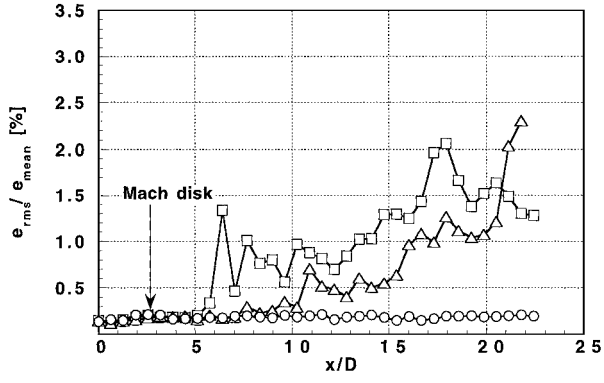

Fig. 3 Hot-wire voltage fluctuation on the center line (●, Re_d = 3.9×10^3; △, $Re_d = 7.7 \times 10^3$; □, $Re_d = 11.6 \times 10^3$).

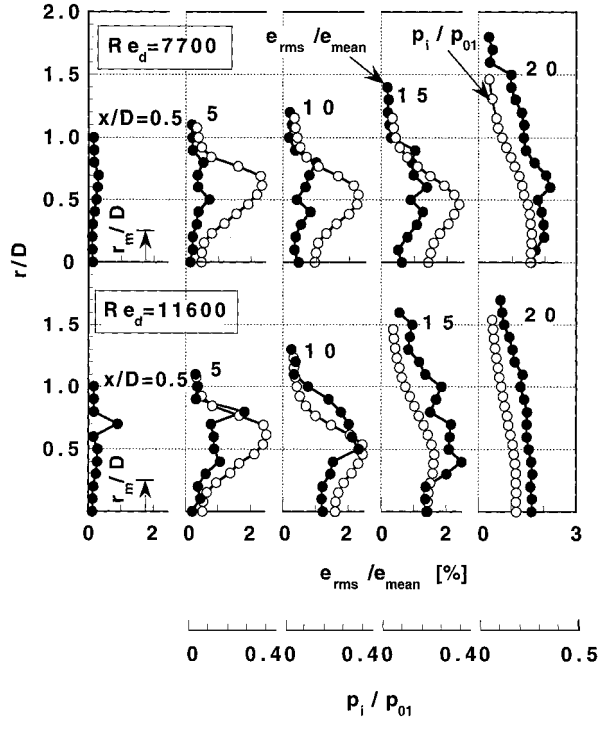

Fig. 4 Radial distributions of hot-wire voltage fluctuation.

of the Mach disk ($x/D = 5$), the fluctuation data take two maximums where the gradient of the radial pitot-pressure distribution is close to the maximum values. Considering the radial pitot-pressure distribution and the Mach disk radius, the locations of these two maximums correspond to the jet boundary and the slip surface originating from the triple point, respectively. Similar results were obtained by Masuda et al.[7] and Miles et al.[8] The fluctuation generated in these two locations then merge at $x/D > 15$. This behavior of the fluctuation also seems to substantiate that the turbulent momentum transfer is the main mechanism of the pitot-pressure recovery.

IV. Conclusions

The pitot-pressure distributions were studied for the underexpanded jets issuing from axisymmetric supersonic nozzle with a design Mach number of 2.0. The pressure ratio was 20, and the Reynolds number based on the nozzle-exit conditions was 3.9×10^3, 7.7×10^3, and 11.6×10^3.

Experiments by the hot-wire probe show that the flow is laminar for $Re_d = 3.9 \times 10^3$, but it is turbulent for $Re_d = 7.7 \times 10^3$ and 11.6×10^3. In both flows the pitot pressure is found to recover downstream of the Mach disk. In the laminar jet the pitot pressure recovered gradually. This slow recovery is attributable to the viscous effect that transfers momentum from the high total pressure peripheral to the low total pressure central region of the jet. For the turbulent jet, on the other hand, the significant recovery of the pitot pressure is observed. In this jet, the hot-wire probe measurements detected the fluctuation originating near the slip surface formed by the triple point at the stem of the Mach disk. This fluctuation developed in the downstream and reached the jet center, from where the pitot pressure was observed to recover; this suggests that the large pitot-pressure recovery is caused by the turbulent momentum transfer from the high total pressure region outside the slip surface to the central core region.

Acknowledgment

The authors would like to express their thanks to H. Yano for his assistance in the experimental work.

References

[1]Moskal, T. E., Bunton, M. A., and Jordan, C. A., "Results of Laboratory Testing and Field Trials of Improved Sootblower Nozzles," *TAPPI 1993 Engineering Conference Proceedings*, Vol. 3, Tappi Press, Atlanta, 1993, pp. 963–967.

[2]Troutt, T. R., and McLaughlin, D. K., "Experiments on the Flow and Acoustic Properties of a Moderate-Reynolds-Number Supersonic Jet," *Journal of Fluid Mechanics*, Vol. 116, 1982, pp. 123–156.

[3]Shen, H., and Tam, C. K. W., "Numerical Simulation of the Generation of Axisymmetric Mode Jet Screech Tones," *AIAA Journal*, Vol. 36, No. 10, 1998, pp. 1801–1807.

[4]Foelsch, K., "The Analytical Design of an Axially Symmetric Laval Nozzle for a Parallel and Uniform Jet," *Journal of the Aeronautical Sciences*, Vol. 16, No. 3, 1949, pp. 161–188.

[5]Driftmyer, R. T., "A Correlation of Freejet Data," *AIAA Journal*, Vol. 10, No. 8, 1972, pp. 1093–1095.

[6]Love, E. S., Grigsby, C. E., Lee, L. P., and Woodling, M. J., "Experimental and Theoretical Studies of Axisymmetric Free Jets," NASA TR R-6, 1959.

[7]Masuda, M., Nakamura, H., Matsumoto, Y., Matsuo, K., and Akazaki, M., "Turbulence Measurement of a Low-Density Supersonic Jet with a Laser-Induced Fluorescence Method," *Progress in Astronautics and Aeronautics*, Vol. 117, 1989, pp. 149–156.

[8]Miles, R. B., Connors, J., Markovitz, E., Howard, P., and Roth, G., "Instantaneous Supersonic Velocity Profile in an Underexpanded Sonic Air Jet by Oxygen Flow Tagging," *Physics of Fluids A*, Vol. 1, No. 2, 1989, pp. 389–393.